

# Medium Effect on the Geometric Isomerism of a Centrosymmetrically Disubstituted Naphthalene Derivative with Flexible Methoxytriethylene Glycol Chains

Ioanna Balomenou,<sup>†</sup> Antonia Kaloudi-Chantzea,<sup>†</sup> Georgios Bokias,<sup>§</sup> Joannis K. Kallitsis,<sup>§</sup> Catherine P. Raptopoulou,<sup>‡</sup> Aris Terzis,<sup>‡</sup> and George Pistolis<sup>\*,†</sup>

NCSR “Demokritos” Institute of Physical Chemistry and, Institute of Materials Science, 153 10 Athens, Greece, Department of Chemistry, University of Patras, 26504 Patras, Greece

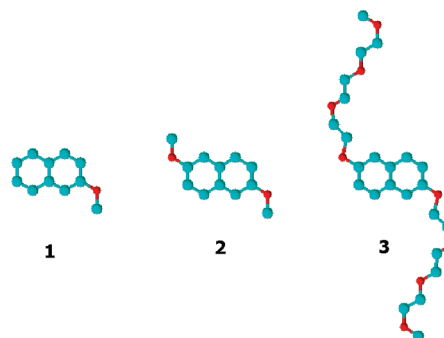
Received: April 6, 2010; Revised Manuscript Received: May 17, 2010

The geometric isomeric diversity of a centrosymmetrically disubstituted naphthalene derivative with flexible methoxytriethyleneglycol chains has been investigated both in the liquid and the solid state. Owing to the fact that the exocyclic C<sub>ArYL</sub>–O linking appears to be essentially a double bond, the material can exist in discrete geometric isomers. Variable temperature ultraviolet absorption and fluorescence spectroscopy combined with single crystal X-ray diffraction reveal the nature of the various stereoisomers present in the liquid and solid phase. Computational support is also given wherever possible. In solution, the material exists predominantly as a mixture of two rapidly interconverting stereoisomers; namely, the thermodynamically preferred *cis*, *cis* and the energetically closest lying *cis*, *trans* configuration. In the solid state, optical spectroscopic methods provide evidence for the presence of a small amount of the energetically highly unstable *trans*, *trans* stereoisomer, kinetically trapped in the lattice defined by the scaffold of the predominant *cis*, *cis* isomeric form. Unlocking of the seemingly frozen *cis*, *cis* ⇌ *trans*, *trans* equilibrium was observed in the molten state.

## Introduction

The influence of the medium on the geometric isomerism (*cis*–*trans*) of organic molecules is a topic receiving growing interest in a wide range of fields in chemistry spanning from gas phase<sup>1</sup> to fluid<sup>2</sup> and glassy solutions, crystals,<sup>3</sup> cavitands,<sup>4</sup> and proteins.<sup>5</sup> The various isomers of a qualified compound, in the ground state and in noninteracting solvents, equilibrate thermally, and normally, their relative populations are determined approximately by the Boltzmann’s distribution law. When equilibrating stereoisomers of a given compound differ considerably in energy in solution, crystallization usually leads to a solid state structure in which the most stable conformation predominates. Occasionally, in some packing motifs of the solid state assemblies associated with specific stabilizing supramolecular interactions, more than one conformer may coexist.<sup>6</sup> Seldomly, different conformers of similar overall molecular shapes may be distributed randomly throughout the solid lattice. In such a case, the relative populations of the conformers are regulated by the relative intermolecular and intramolecular energies involved.<sup>6</sup> In cases that X-ray diffraction analysis cannot unambiguously distinguish the coexistence of two or more isomers of a certain organic dye in the same crystal lattice, photophysical methods appear to be by far the most relevant tools. For instance, the two major decay processes for excited rhodopsin have been recently explained satisfactorily by suggesting the presence of two noninteracting ground state rotameric forms of the 11-*cis*-retinyl.<sup>7</sup> The simultaneous existence of two rotamers in the ground state, one of which was not observed in the X-ray structure, has been suggested experimen-

## SCHEME 1: Structures of Compounds under Discussion: (1) 2-Methoxynaphthalene; (2) 2,6-Dimethoxynaphthalene, and (3) an Analogue of 2 Modified with Methoxytriethylene Glycol Oligomeric Chains



tally<sup>8,9</sup> and supported computationally<sup>10</sup> for tryptophan (Trp) in the environment of biological macromolecules.

It has been established that substituted naphthalene derivatives with flexible oligomeric ethyleneglycol chains can be used as important functional substrates in several exciting fields of current scientific research. For example, these derivatives are widely used to link together functional components in artificial molecular machines;<sup>11</sup> they also find use as agents in templated supramolecular polymerization.<sup>12</sup> It is therefore interesting and useful to obtain a comprehensive study on this class of compounds to elucidate possible conformational diversity in various media.

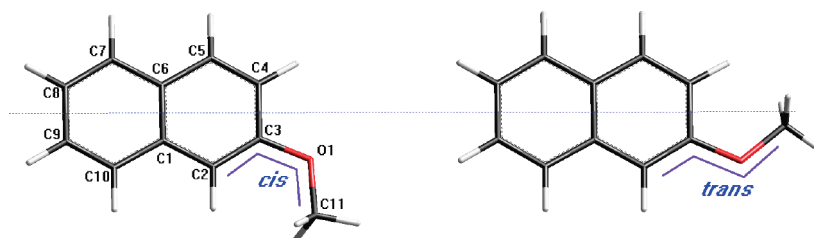
With this in mind, we have synthesized the naphthalene derivative (3) as a representative compound in which two methoxytriethylene glycol chains have been attached centrosymmetrically at the 2,6- position of the aromatic moiety (scheme 1). We report herein on the conformational diversity of 3 in

\* Corresponding author. E-mail: pistolis@chem.demokritos.gr.

<sup>†</sup> NCSR “Demokritos” Institute of Physical Chemistry.

<sup>§</sup> University of Patras.

<sup>‡</sup> Institute of Materials Science.

**SCHEME 2: Conformational Isomers of 1: The Cis (syn,  $\varphi \approx 0^\circ$ ) and Trans (anti,  $\varphi \approx 180^\circ$ ) Configurations Are Denoted by the Dihedral Angle  $\varphi$  Formed by the Naphthalene Plane and the O-Me Bond Vector,  $\varphi(\text{C2}-\text{C3}-\text{O1}-\text{C11})$** **TABLE 1: Selected Geometrical Parameters of Cis and Trans Isomers of Methoxynaphthalene (1) Obtained by Theory (DFT and RHF) and X-ray Analysis (cis form)<sup>a</sup>**

	cis		trans		crystal structure (cis form) <sup>15</sup>
	DFT	RHF <sup>b</sup>	DFT	RHF	
C1–C2	1.429	1.426 (1.425)	1.421	1.414	1.427
C2–C3	1.390	1.360 (1.360)	1.393	1.365	1.378
C3–C4	1.426	1.423 (1.423)	1.424	1.416	1.421
C4–C5	1.381	1.354 (1.352)	1.388	1.363	1.363
C5–C6	1.430	1.426 (1.424)	1.424	1.415	1.426
C6–C7	1.425	1.418 (1.417)	1.427	1.422	1.419
C7–C8	1.388	1.363 (1.360)	1.386	1.358	1.374
C8–C9	1.420	1.414 (1.413)	1.423	1.420	1.415
C9–C10	1.388	1.363 (1.360)	1.386	1.359	1.374
C10–C1	1.428	1.420 (1.419)	1.430	1.426	1.425
C1–C6	1.440	1.405 (1.407)	1.443	1.408	1.423
C3–O1	1.374	1.349 (1.347)	1.377	1.353	1.375
O1–C11	1.431	1.404 (1.399)	1.430	1.403	1.425
$\varphi(\text{C3}-\text{O1}-\text{C11})$	117.4	119.3 (119.5)	117.9	120.0	117.2
$\varphi(\text{C2}-\text{C3}-\text{O1})$	125.5	125.6 (125.5)	116.0	116.8	125.1
$\varphi(\text{C2}-\text{C3}-\text{O1}-\text{C11})$	0.0	0.0	179.0	178.6	-3.2
relative energies of conformers (kJ/mol)	0.0	0.0	5.9	6.0 (8.4)	

<sup>a</sup> Lengths in angstroms and torsions in degrees. <sup>b</sup> Entries in parentheses are taken from ref 13b at the RHF/6-31G\*\* level.

both the fluid phase and the solid state. We also include in our study, wherever appropriate and helpful, the precursory compound **2** and its singly substituted derivative **1**.

## Results and Discussion

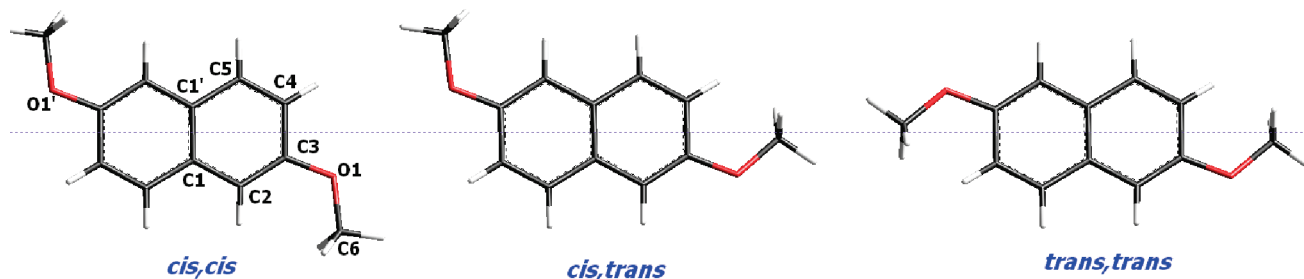
**I. Analysis of the Geometric Isomers.** There is sufficient evidence in the recent literature that 2-methoxynaphthalene (**1**) exhibits geometric isomerism via rotation about the  $\text{C}_{\text{Aryl}}-\text{O}$  quasi-single bond both in the gas phase<sup>13</sup> and the solution.<sup>14</sup> Two ground state isomers were found to exist in the gas phase and have been assigned to a cis (syn,  $\varphi = 0^\circ$ ) and a trans (anti,  $\varphi = 180^\circ$ ) configuration (see Scheme 2). This assignment has been also supported computationally<sup>13b</sup> at the RHF/6-31G\*\* level of theory. Single crystal X-ray diffraction analysis proves that **1** crystallizes as a nearly planar molecule with the methoxy group adopting the syn-periplanar conformation (cis) with respect to C2 atom<sup>15</sup> (see also Table 1). Furthermore, we have recently demonstrated that 2-methoxynaphthalene (**1**) in the liquid phase (3-methylpentane; 3-MP) can exist in two different spectrally distinct conformations, cis (syn) and trans (anti), which may interconvert torsionally (around the  $\text{C}_{\text{Aryl}}-\text{O}$  “double” bond by  $180^\circ$ ) both thermally and photochemically.<sup>14</sup> From the observed temperature dependence of the absorption spectrum, we estimated an enhanced stability of  $\approx 6.0$  kJ/mol ( $\sim 500$   $\text{cm}^{-1}$ ) of the cis configuration in the electronic ground state.

To compare and substantiate our experimental results more accurately for the singly and disubstituted derivatives **1** and **2**, we calculated here fully relaxed torsional potential with the restricted Hartree–Fock RHF and density functional theories DFT methodologies (the latter using the PBE96 exchange correlation potential) combined with the cc-pVDZ Dunning

correlation-consistent basis set.<sup>16</sup> Further, diffuse functions (aug)-cc-pVDZ were added to oxygen. The geometries were optimized initially at the RHF/ (aug)-cc-pVDZ level. Subsequently, single point calculations were carried out with the electron correlation correction by the second-order Møller–Plesset perturbation method (MP2) by the second-order Møller–Plesset perturbation method (MP2) for the optimized geometries (MP2//RHF/(aug)-cc-pVDZ).

The present calculations, indeed, give two minima on the potential energy surface of **1** in the ground state; these correspond to the structures depicted in Scheme 2. The calculated geometrical parameters of the two isomeric structures are shown in Table 1 and are compared with those obtained from crystallographic analysis and previous calculations. Both methods (MP2//RHF and DFT) predict the cis configuration to be the lowest energy structure, which is consistent with the prediction of a previous ab initio study at the RHF/6-31G\*\* level.<sup>13b</sup> Furthermore, the above configuration closely resembles the structure found in the X-ray analysis.

Although no symmetry constraints were applied, deviations from planarity of the equilibrium geometries of the isolated molecule are found to be negligible (for example,  $\varphi(\text{C2}-\text{C3}-\text{O1}-\text{C11}) \approx 0^\circ$ , cis; and  $\approx 180^\circ$ , trans), yielding an approximate  $\text{C}_s$  molecular point group for both structures. All methods predict that (a) the angle  $\varphi(\text{C3}-\text{O1}-\text{C11})$  nearly matches the unperturbed one ( $120.0^\circ$ ) of a perfectly  $\text{sp}^2$  hybridized atom and (b) the O1–C11 bond lies almost in the plane of the naphthalene ring (planar  $\text{C}_s$  symmetry for both isomers). The above suggest significant interactions between the naphthalene’s orbitals and the oxygen’s lone electron pair lying perpendicular to the aromatic plane. Accordingly, the exocyclic C3–O1 linking appears to be essentially a double bond in both configurations

SCHEME 3: Geometric Isomers of **2** and **3**TABLE 2: Selected Geometrical Parameters of Cis, Cis; Cis, Trans; and Trans, Trans Isomers of Dimethoxynaphthalene (**2**) Obtained by Theory (MP2//RHF/(aug)-cc-pVDZ) and X-ray Crystal Structure of **3** (cis, cis form) (angstroms and degrees)

	cis, cis	cis, trans	trans, trans	X-ray analysis of <b>3</b> (cis, cis form)
C1–C2	1.424	1.411 (1.428)	1.416	1.419
C2–C3	1.361	1.366 (1.357)	1.361	1.373
C3–C4	1.419	1.412 (1.425)	1.419	1.417
C4–C5	1.357	1.366 (1.353)	1.362	1.357
C5–C1'	1.423	1.412 (1.429)	1.418	1.417
C1–C1'	1.400	1.404	1.407	1.418
C3–O1	1.352	1.356 (1.352)	1.356	1.366
O1–C6	1.403	1.402 (1.403)	1.402	1.426
$\varphi(\text{C3–O1–C6})$	119.3	119.7 (118.9)	120.2	118.3
$\varphi(\text{C2–C3–O1})$	125.9	116.8 (125.8)	116.8	125.6
$\varphi(\text{C2–C3–O1–C6})$	–0.1	180.0 (0.0)	180.0	6.7
relative energies of isomers (kJ/mol)	0	4.9	11.5	

<sup>a</sup> Entries in parentheses give the centrosymmetrically related value in the other half of the molecule.

(cis and trans) with a length (1.374 Å; see Table 1) significantly shorter than a typical single C–O bond length (1.43 Å in methyl ether<sup>17</sup>).

The computational methods employed here (namely, DFT and MP2//RHF) are consistent and predict the two isomers (cis and trans) to differ in energy by 5.9 kJ/mol (493 cm<sup>–1</sup>) and 6.0 kJ/mol (502 cm<sup>–1</sup>), respectively. These estimates are in excellent agreement with the ground state energy gap between the two isomeric forms of **1** derived experimentally  $\Delta H^{S0} \approx 6.0$  kJ/mol ( $\sim 500$  cm<sup>–1</sup>) in 3-MP. It should be pointed out that the above calculated values are found to be remarkably higher (7.3 kJ/mol, RHF/(aug)-cc-pVDZ; 8.4 kJ/mol, RHF/6-31G\*\*) when electron correlation effects (MP2) are ignored. The energy gap between the equilibrium geometries of the two isomers in the ground state could be primarily attributed to the unequal steric repulsions between the closest lying hydrogens attached to the naphthalene subunit and methyl group, respectively. More details on the kinetics and thermodynamics of the isomeric interconversion in the ground and the first excited states are given elsewhere.<sup>14</sup>

For the centrosymmetrically disubstituted derivative **2** (2,6-dimethoxynaphthalene), the present calculations yielded three minima on the potential energy surface of the ground state. These minima correspond to the structures depicted in Scheme 3. Because of difficulties encountered with the convergence criterion in DFT methods, we have employed only the MP2//RHF/(aug)-cc-pVDZ level of theory for compound **2**. The calculated geometrical parameters of the three conformational isomers are shown in Table 2 and are compared with the core geometry obtained from the available crystal structure of **3** (see X-ray Crystallography). The calculations predict the cis, cis configuration to be the lowest energy structure (global minimum) closely resembling the core structure of **3** found from the X-ray analysis.

All geometric isomers of the isolated molecule **2** are predicted to be strictly planar, albeit in the crystal structure of **3** (cis, cis

form), a weak deviation from planarity was found [ $\varphi(\text{C2–C3–O1–C11}) \approx 6.7^\circ$ ]. This is not unexpected, considering the fact that conformers in crystal lattices can have somewhat different torsional angles (compared with the gas-phase minimized structures) due to crystal packing forces.<sup>6</sup> The calculations yielded centrosymmetrical structures of approximately  $C_{2h}$  point group symmetry for both the cis, cis and the trans, trans forms. In contrast, the planar cis, trans configuration possess a lower symmetry,  $C_s$ , with remarkable differences in the bond lengths between the two halves of the naphthalene ring (see Table 2). In all structures, the oxygen atoms are sp<sup>2</sup> hybridized, giving a double-bond character to the C3–O1 bond that connects the methoxy group to the naphthalene subunit (1.352–1.356 Å at the RHF level; 1.366 Å from X-ray). Finally, the equilibrium geometries (local minima) of the cis, trans and trans, trans isomers are found to lie higher in energy with respect to the global minimum (cis, cis configuration) by 4.9 ( $\sim 410$  cm<sup>–1</sup>) and 11.5 ( $\sim 962$  cm<sup>–1</sup>) kJ/mol respectively.

**II. Solution Photophysics.** The temperature dependence of the absorption spectrum of the disubstituted derivative **2** in 3-MP is very closely related to that observed for the singly substituted compound **1**. We note that for compound **1**, only two isomeric forms (cis and trans) can exist in thermal equilibrium (Figure 1a). The presence of several isosbestic points across the absorption spectrum of **2** when the sample is cooled stepwise from 296 to 77 K provides evidence for the presence in the ground state of two discrete isomeric forms in thermal equilibrium; namely, the predominant thermodynamically stable cis, cis (**A**) and the energetically closest lying cis, trans (**B**) form.

Indeed, the low temperature (77 K) absorption spectrum of **2** (i.e., the thermodynamically stable form) very closely resembles that of the cis, cis (**A**) isomer, the sole observed in the X-ray analysis of crystals of the analogue compound **3** (see Scheme 4). Furthermore, a plot of  $\ln K$  vs  $1/T$  for the ground state equilibration of the above isomers gives an estimate of  $\Delta H^{S0} \approx 5$  kJ/mol that is exceptionally consistent with that

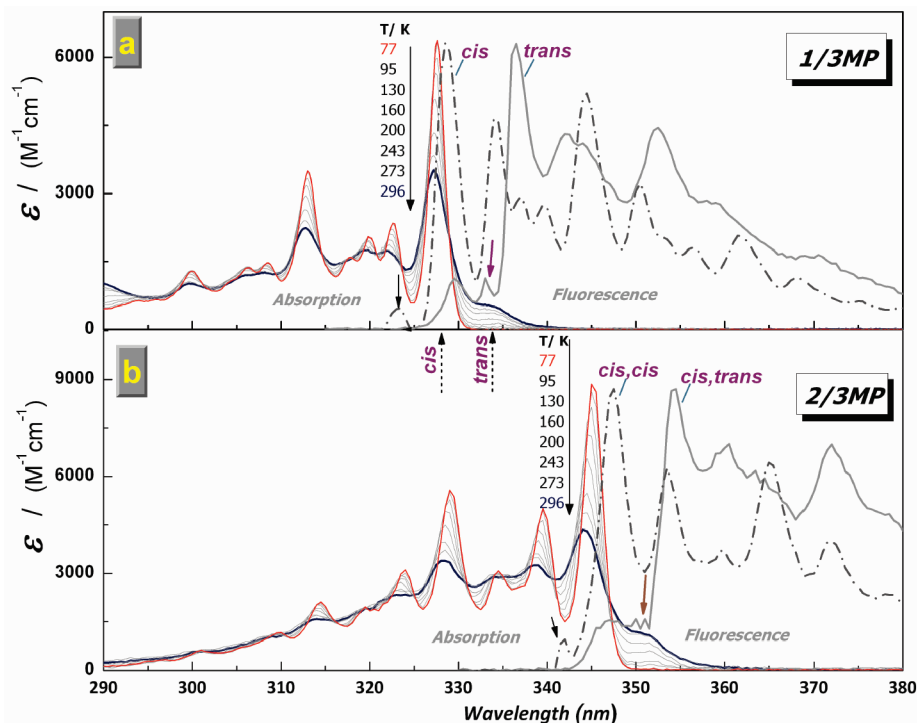
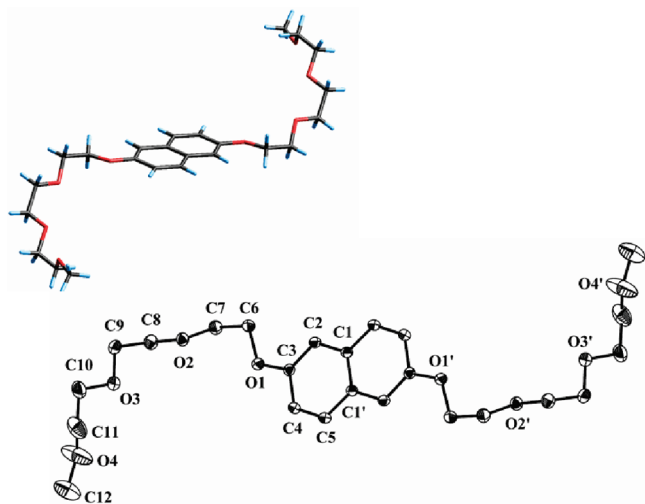


**Figure 1.** Left: Absorption spectra of **1** (upper panel) and **2** (lower panel) in 3-MP at varying temperatures corrected for temperature dependence of the density of the solution.<sup>14</sup> Right: Normalized pure fluorescence spectra of isomeric forms of **1** and **2** in 3-MP obtained by selective excitation (see solid arrows). Scattered excitation light has been removed.

**SCHEME 4: Molecular Unit and Partially Labelled ORTEP Plot of **3** with Ellipsoids Drawn at the 30% Probability Level<sup>a</sup>**



<sup>a</sup> Hydrogen atoms have been omitted for clarity. Primed atoms are generated by symmetry ( $' = 2-x, -y, 2z$ ).

predicted from theory (4.9 kJ/mol) for the ground state energy gap between the cis, cis and cis, trans isomeric forms (see inset Figure 2 and the Supporting Information, part S2). The energetically highly unfavorable trans, trans isomer was not clearly observed spectroscopically due to its very low abundance ( $\sim 1\%$  according to the Boltzmann's distribution law).

It should be pointed out that because compound **3** is insufficiently soluble in glassy solution of 3-MP, only the spectra of the precursory compound **2** have been recorded at low temperatures. We did not expect appreciable spectral differences between **2** and **3**. To prove this hypothesis, we investigated comprehensively the photophysics of the compounds under

discussion dissolved in 2-methyltetrahydrofuran (2-MTHF) in which all naphthalene derivatives are readily soluble. 2-MTHF is a noninteracting solvent that forms a high-quality glassy solution at 77 K. The absorption–fluorescence spectra and details in spectral analysis are given in Figure S2–1 of the Supporting Information.

The photophysical properties of the distinct isomers of all compounds are collected in Table 3 and lead to the following conclusions: (1) There is nearly perfect mirror symmetry between the low temperature absorption and emission spectrum; both display vibronic features that correlate very well with that of the corresponding parent naphthalene molecule.<sup>13</sup> (2) The electronic spectra of the disubstituted derivatives **2** and **3** are found to be shifted bathochromically by  $\sim 20$  nm with respect to the singly substituted derivative **1**, regardless of the solvent's quality.<sup>18</sup> These spectral differences could be attributed to the additive conjugative effect induced by the C6 attachment of a second GO– group ( $G = \text{Me}$ , **2** or  $G = \text{C}_7\text{H}_{15}\text{O}_3$ , **3**). (3) The radiative rate constants determined experimentally are in accordance with those calculated using the Strickler–Berg formulation.<sup>19</sup> This indicates that the emission is an allowed process originating from a  $\pi\text{--}\pi^*$  singlet excited state, as has been demonstrated experimentally<sup>13b</sup> and supported from theory<sup>13a</sup> for the simple derivative **1**. (4) It is important to note that the photochemically inert oligomeric chains of **3** do not affect the photophysical properties of the aromatic core or the relative energies of the stereoisomers differently from the methoxy groups of the precursory compound **2**. In summary, the above findings conclusively demonstrate that the spectrally distinguishable geometric isomers of the compounds under study have very closely related photophysical properties that are not altered by environmental stimuli, such as a solvent's dielectricity, proticity, and viscosity<sup>18</sup> (see also Table 3).

**III. X-ray Crystallography.** Single crystals of **3** were obtained via slow evaporation of a solution of **3** in a mixture

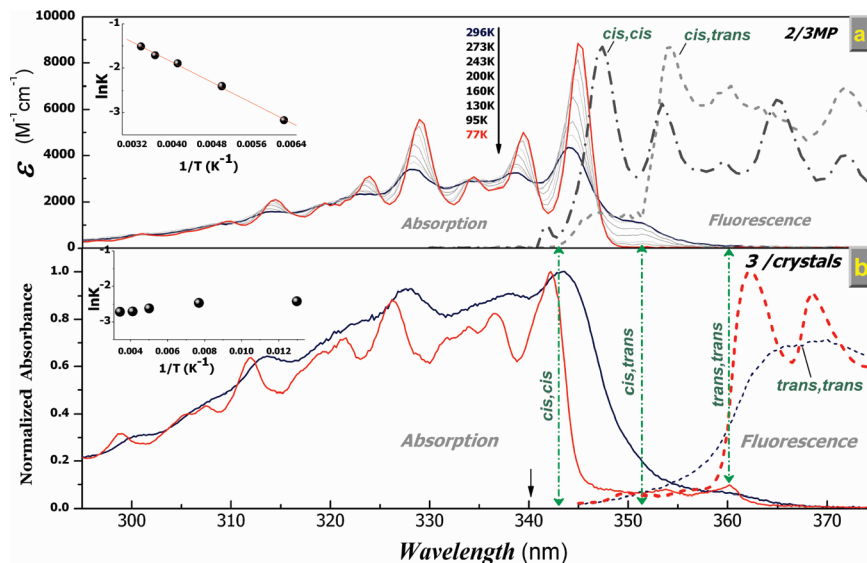


**Figure 2.** (a) As in Figure 1b (absorption and pure fluorescence spectra of isomeric forms of **2** dissolved in 3-MP at varying temperatures); (b) Normalized absorption (left) and fluorescence spectra of a crystalline film of **3** (right; exc:  $340.2 \pm 0.1$  nm) obtained at ambient and low temperature (see text for details). Insets:  $\ln K$  vs  $1/T$  for the ground state interconversion between: (upper) the cis, cis and cis, trans isomers of **2** in 3-MP and (down) cis, cis and trans, trans isomers in crystals.  $K$  is the ratio of the minor population to that of the major.

**TABLE 3: Fluorescence Quantum Yields ( $\Phi$ ); Lifetimes ( $\tau$ ); Radiative Rates Constants,  $k_f$  and  $k_f^{\text{SB}}$ , Obtained, Respectively, Experimentally and from the Strickler–Berg Formulation; Non-Radiative Rates Constants ( $k_{\text{nr}}$ ); Maxima of the Transition Origins,  $\nu_{\text{max abs}}$ ; Differences between Maxima of the Transition Origins  $\Delta\nu_{\text{max}}^{\text{abs}}$  and Oscillator Strengths,  $f$ , of the Geometric Isomers of Compounds **1**, **2**, and **3** Obtained at Low Temperatures in 3-Methylpentane (3-MP) and 2-Methyltetrahydrofuran (2-MTHF)**

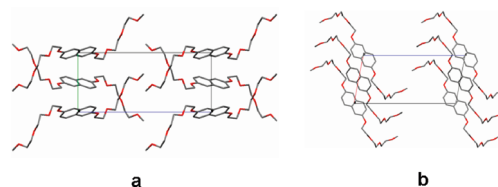
molecule	solvent	isomer	$\Phi^a$	$\tau$ (ns) <sup>b</sup>	$k_f$ , $10^7$ (s <sup>-1</sup> ) <sup>b</sup>	$k_f^{\text{SB}}$ , $10^7$ (s <sup>-1</sup> )	$k_{\text{nr}}$ , $10^7$ (s <sup>-1</sup> ) <sup>b</sup>	$\nu_{\text{max abs}}$ (cm <sup>-1</sup> )	$\Delta\nu_{\text{max abs}}$ (cm <sup>-1</sup> )	$f$
<b>1</b>	3MP	cis	0.36	13.0	2.90	2.88	4.80	30 520	0	0.017
		trans	0.40	13.0	2.90	2.88	4.80	29 985	535	
	2MTHF	cis	0.39	12.7	3.07	3.81	4.80	30 413	0	0.019
		trans	0.41	12.2	3.36	4.84	4.84	29 760	650	
<b>2</b>	3MP	cis, cis	0.36	8.6	4.18	4.59	7.44	28 960	0	0.0313
		cis, trans	0.41	8.6	4.77	6.86	6.86	28 450	510	
	2MTHF	cis, cis	0.34	8.1	4.20	4.99	8.14	28 818	0	0.033
		cis, trans	0.39	8.5	4.59	7.17	7.17	28 246	572	
<b>3</b>	2MTHF	cis, cis	0.35	8.1	4.32	4.89	8.02	28 818	0	0.032
		cis, trans	0.40	8.6	4.65	6.98	6.98	28 246	572	

<sup>a</sup> Uncertainties in low temperature quantum yields,  $\sim 10\%$ . <sup>b</sup> Uncertainties in recovered lifetimes and rate constants,  $\sim 5\%$  and  $\sim 10\%$ , respectively.

of chloroform and *n*-heptane and were verified to be stable for several months. The crystal structure of **3** was solved by single-crystal X-ray diffraction in the monoclinic space group  $P2_1/\alpha$ . The analysis reveals that compound **3** is centrosymmetric, and the inversion center is in the middle of the  $\text{C1}\cdots\text{C1}'$  bond (Scheme 4).

The data show that the  $\text{O1}-\text{C6}$  bond lies almost in the plane of the naphthalene ring (dihedral angle  $\varphi(\text{C}_2-\text{C}_3-\text{O}_1-\text{C}_6) = 6.7^\circ$ ) adopting the syn-periplanar conformation (cis, cis configuration). In contrast, each oligomeric chain (methoxytriethylene glycol moiety) is folded markedly out-of-plane of the naphthalene ring, forming a criss-cross-like arrangement with an adjacent chain. The asymmetric unit contains two crystallographically independent half molecules, each lying on a crystallographic inversion center, as seen in Scheme 5. A close inspection of the dimeric unit (scheme 6) shows that the planar subunit (aromatic core) of the molecule is stabilized by the presence of strong intermolecular  $\text{C}-\text{H}\cdots\text{O}$  aromatic (2.686 and 2.968 Å) and weaker aliphatic  $\text{C}-\text{H}\cdots\pi$  ( $\sim 3$  Å) interactions. The folded-chain conformation is further stabilized with aliphatic  $\text{C}-\text{H}\cdots\text{O}$  (2.652 and 2.890 Å) interactions with an adjacent oligomeric chain. No  $\pi-\pi$  stacking between two

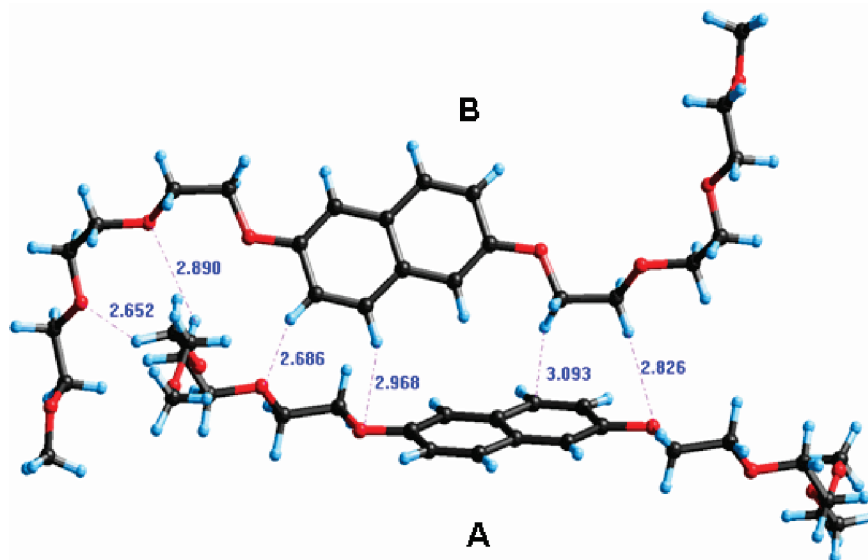
**SCHEME 5: Crystal Packing of **3** Viewed Down (a) Alpha and (b) Beta Crystallographic Axes<sup>a</sup>**



<sup>a</sup> Hydrogens atoms have been omitted for clarity.

closest-lying aromatic rings was observed in the crystal. The crystal analysis reveals that the aromatic subunits of the alternate molecules are translated (slipped) noticeably along the long naphthalene axis relative each other. The absence of  $\pi-\pi$  stacking is also evident from the strong deviation from planarity between two adjacent aromatic planes ( $\sim 60^\circ$ ) and their long centroid–centroid distance ( $\sim 5.4$  Å).

**IV. Solid State Photophysics.** After several attempts, we were able to obtain a thin crystalline film of appropriate quality for UV–vis transmittance spectroscopy; the preparation was made by deposition on a quartz plate via slow evaporation of a solution of **3** in a mixture of chloroform/*n*-decane. The absorp-

SCHEME 6: Interactions (Å) between Two Crystallographically Independent Molecules Taken from the X-ray Analysis<sup>a</sup>

<sup>a</sup> Carbon, black; oxygen, red; hydrogen, cyan.

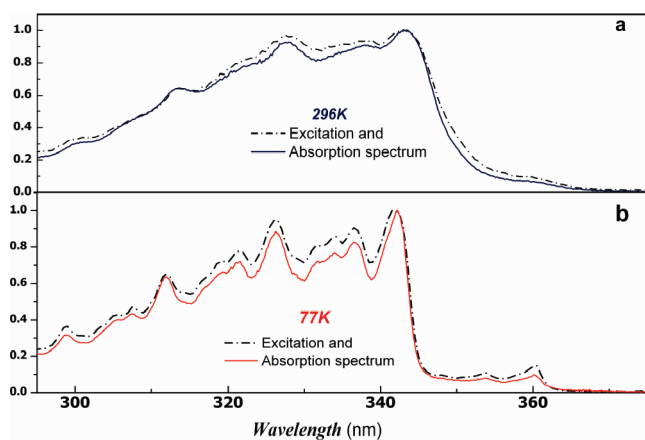


**Figure 3.** Normalized absorption and fluorescence excitation spectra of a crystalline film of **3** at 296 and 77 K, respectively.

tion, fluorescence, fluorescence excitation spectra, and fluorescence lifetimes have been monitored over a wide temperature range, and the most interesting aspects are discussed below.

As seen in Figure 2b, the absorption spectrum is governed predominantly by the *cis, cis* isomer, the sole observed in the X-ray analysis of crystals; it closely resembles that of the thermodynamically favored isomeric form monitored in a glassy solution at 77 K, confirming essentially that the *cis, cis* isomer is the energetically stable form in solution in agreement with theory. The transmittance absorption spectrum and the emission wavelength-dependent excitation spectrum of the film (monitored with front face geometry) are essentially superimposable (see Figure 3). This experimental fact clearly demonstrates the quality and the suitability of the crystalline film for optical transmittance spectroscopy. Notice also that the excitation/fluorescence spectra of the film coincide with the corresponding ones of a single crystal.

Interestingly, in the above spectra, the presence of a minor subpopulation of a distinct species **C** becomes apparent in the crystal lattice of the predominant *cis, cis* form. As seen, the maximum of the first electronic transition of **C** is shifted distinctly bathochromically ( $\lambda_{\text{max}} \sim 360$  nm;  $\sim 27777$   $\text{cm}^{-1}$ ) by  $\sim 1240$  and  $\sim 635$   $\text{cm}^{-1}$  as compared with those of the *cis, cis* and *cis, trans* isomeric forms of **2**, respectively, in 3-MP.

The ratio of the optical densities at the absorption maxima of the **C** and *cis, cis* species ( $\sim 360$  and  $\sim 343$  nm, respectively) remains constant ( $\text{OD}_{\text{C}}^{0-0}/\text{OD}_{\text{A}}^{0-0} \sim 0.06$ ) with temperature (77–300 K), suggesting no thermal interconversion between the above species in the crystal lattice. In contrast to the liquid phase, emission of the predominant *cis, cis* isomer in crystals cannot be detected at all; instead, the emission spectrum is actually independent of the excitation wavelength and shows perfect mirror symmetry with the absorption spectrum of **C**, as clearly manifested by the absorption, fluorescence and fluorescence excitation spectrum (Figure 2b and 4). Moreover, the fluorescence intensity decays strictly monoexponentially; the recovered fluorescence lifetimes are minimally affected by temperature (9.1 and 11.1 ns at 300 and 77 K, respectively) and are similar to the ones recovered for the isolated *cis, cis* and *cis, trans* isomeric units in dilute solutions (see Table 3).

One may be inclined to believe that the long wavelength absorbance is due to an impurity. This possibility, however, must be excluded. When, for example, the crystals are dissolved in an inert solvent, the absorption spectrum recovers its typical shape and follows the temperature dependence discussed previously in detail. In addition, the differential scanning calorimetry (DSC) thermograph of crystalline **3** yields a single sharp endotherm at 86.4 °C and a sharp exothermic peak upon cooling at 80.0 °C (recrystallization from the supercooled melt; see Figure 5 inset). Furthermore, the combined steady-state and time-resolved experiments clearly demonstrate the absence of quenching sites in the crystal lattice. In other words, the species **C** could not be attributed to an aggregated site. It should be pointed out that aggregation phenomena in the solid state usually give rise to complex multiexponential fluorescence decay profiles and to broad, structureless, and red-shifted excimer-like emission bands.<sup>20</sup>

In obvious contrast to the fluid phase in which the material exists as a mixture of rapidly interconverting *cis, cis* and *cis, trans* isomers, the above findings clearly prove that a small amount of a kinetically trapped stereoisomer of **3** is distributed randomly throughout the crystal lattice of the energetically preferred *cis, cis* isomeric form. Given the spectral insensitivity of the *cis, cis* and *cis, trans* isomers of **3** (and **2**) to various environmental stimuli, the above isomeric form **C** (spectroscopi-

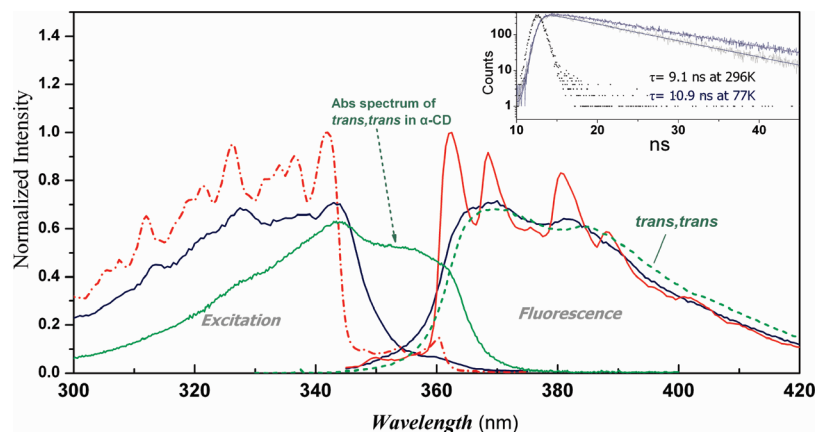


**Figure 4.** Green curves: Normalized absorption and emission spectrum of the *trans, trans* form of **2** trapped supramolecularly within the nanospace formed by two assembled  $\alpha$ -cyclodextrins in aqueous solution. Normalized fluorescence (exc: 337 nm) and fluorescence excitation spectra of a thin crystalline film of **3** at 296 (blue) and 77 K (red), respectively.

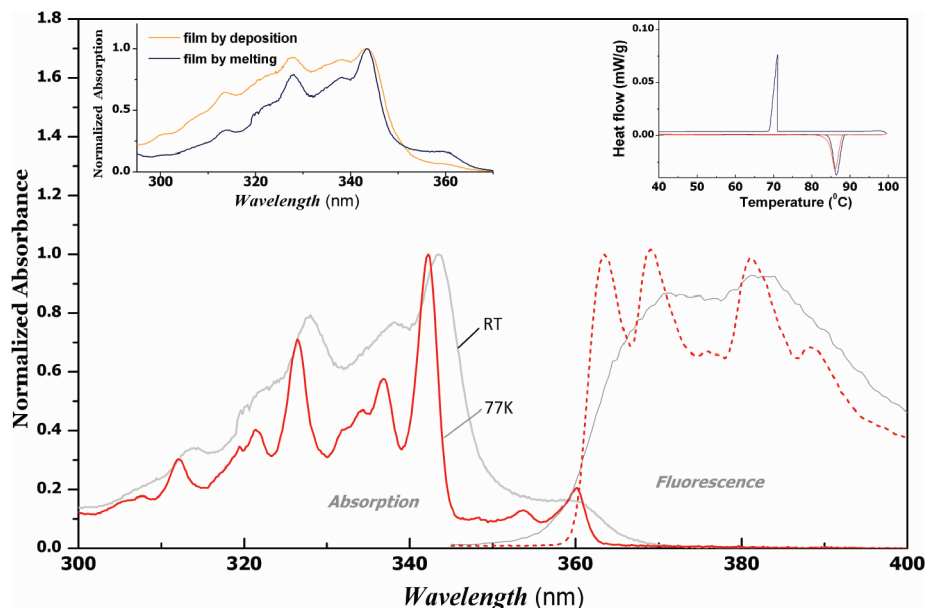


**Figure 5.** Normalized absorption and emission spectra of a film obtained by the melting method. Insets: (left) Absorption spectra of films obtained with the deposition and melting method respectively (see text for details); (right) differential scanning thermograph of solid **3** (a heat-cool-heat sequence).

cally quite distinguishable from the aforementioned configurations) should uniquely represent the *trans, trans* stereoisomer, as is manifested experimentally and is supported also computationally. Specifically, we recently provided clear evidence by optical and  $^1\text{H}$  NMR spectroscopic methods that a suitably sized/shaped cavitand ( $\alpha$ -cyclodextrin) demonstrated pure thermodynamic selectivity toward encapsulation of the unstable *trans, trans* form over the other equilibrating analogues (i.e., the *cis, cis* and *cis, trans* isomers) in aqueous solution.<sup>4</sup> Hence, we were able to purely isolate and permanently stabilize the *trans, trans* isomeric form at ambient conditions unmasking, thereby its own electronic spectral features. We recall again that the *trans, trans* stereoisomer is present in only trace amounts in a pure solvent ( $\sim 1\%$ ) and, hence, cannot be clearly observed spectroscopically.

It is clearly seen (Figure 4) that the *trans, trans* form of **2** trapped supramolecularly with  $\alpha$ -cyclodextrin and the **C** form of **3** in crystals have (a) electronic origin transition maxima which nearly coincide ( $\sim 360$  nm) and (b) fluorescence spectra that are essentially superimposable. The above facts strongly suggest that the minor isomeric form **C** in crystals closely resembles structurally the *trans, trans* configuration of **3**. This conclusion is further supported by theory. In particular, singly

excited-state configuration interaction (CI) at the MP2//RHF/aug-cc-pVDZ level of theory predict the  $S_1 \leftarrow S_0$  adiabatic electronic transition origin of the *trans, trans* isomer of **2** to be distinctly shifted bathochromically by  $\sim 1000$  and  $500$   $\text{cm}^{-1}$  with respect to that of the *cis, cis* and *cis, trans* isomer, respectively. The above shifts are almost similar to those we have observed spectroscopically; that is, a red-shifted absorption spectrum of the **C** species in crystals by  $\sim 1230$  and  $\sim 550$   $\text{cm}^{-1}$  relative to the origins of the  $S_1 \leftarrow S_0$  electronic transitions of the aforementioned isomers; namely, *cis, cis* and *cis, trans* configurations (see Figure 2).

In obvious contrast to the uninhibited liquid phase in which the predominant *cis, cis* form equilibrates thermally with the *cis, trans* analogue ( $\sim 82$  and  $\sim 17\%$ , respectively, at room temperature), we see no evidence for the presence of the *cis, trans* isomer in the solid phase. The absence of this form in the solid is not unexpected, considering the fact that (a) certain crystal packing motifs lead to a predominance of one conformation in the crystal structure, whereas in solution, a number of different conformations may be present,<sup>6,21</sup> including ordinarily the one(s) in the crystal structure(s); and (b) the thermal *cis, cis*  $\rightleftharpoons$  *cis, trans* equilibration is prevented, owing to the fact

that strong steric interactions (imposed by the densely packed oligomeric chains of **3** between neighboring molecules) increase prohibitively the energetic barrier for any exocyclic torsional rearrangement(s) (see Schemes 5, 6).

Although the steady-state and time-resolved results could be reasonably rationalized by the simultaneous presence of two subpopulations in the same crystal lattice (namely the major *cis, cis* and the minor *trans, trans*) one would be hard pressed to explain the amplified presence of the latter in the crystals (~6%) as compared with the liquid phase in which it exists in only a trace amount (~1%) before crystallization. We note that the relative abundance of the minor isomer in the crystals of ~6% was made by assuming that the molar extinction coefficient of the *trans, trans* isomer should not differ remarkably with that of the *cis, cis* form.

We believe that the observed cocrystallization might, in fact, be due to specific *supramolecular interactions* during the formation of the critical assembly. In particular, suitable nanospaces formed inside the lattice of the predominant centrosymmetric *cis, cis* isomeric form may have a pronounced effect on the selective trapping and stabilization of the energetically disfavored yet centrosymmetric *trans, trans* stereoisomer. This is not totally unexpected in view of the fact that our recent surprising results clearly demonstrated that supramolecular effects can play a determinant role to stabilize disfavored conformations. Specifically, we provided evidence that control of steric hindrance and tightness in host–guest supramolecular interactions led spontaneously to the *pure* stereoselective trapping, at ambient conditions, of the energetically disfavored *trans, trans* stereoisomer of **2** within the nanospace formed by two self-assembled  $\alpha$ -cyclodextrins.

The literature also makes reference to the situation in which different conformers of similar overall molecular shapes can be randomly distributed throughout the same solid lattice.<sup>6,21</sup> In that case, the relative populations of the conformers can no longer be determined by the Boltzmann's distribution law, but rather, are regulated by the relative intermolecular and intramolecular energies involved. This can be understood by the fact that not all the conformations adopted in crystal structures of conformationally flexible molecules correspond to minima on computed gas phase potential energy surfaces. In other words, ground state deformation(s) imposed by the packing forces (see Solution Photophysics) and, most importantly, specific *supramolecular* interactions between different molecular members during the formation of the critical assembly, can noticeably alter the relative energies of the distinct stereoisomers and, hence, their relative proportion.

**V. Unlocking a Rotary Motion in the Molten Phase.** At this point, we questioned if the melting method was capable of unlocking, at least partially, the frustrated conformations in crystals. To this end, we investigated the effect of loosening the cohesive packing motif of crystals of **3** above its melting point on the thermal equilibration response between the seemingly conformationally frozen isomers (*cis, cis* and *trans, trans*).

Figure 5 shows the normalized absorption and emission spectra of a thin film obtained by heating crystals of **3** above the melting point and then cooling slowly to room temperature. Unfortunately, despite several efforts, we were unable by melt crystallization to obtain crystals of appropriate quality for single crystal X-ray diffraction analysis. However, the strict similarity between the absorption and emission spectral features and the associated photophysics of thin films of **3** (obtained, respectively, from its melt and by the deposition method at room temperature) enable us to conclude that the molecular packing should be the

same in both cases. This conclusion is further supported after careful inspection of the differential scanning thermograph (DSC) of crystalline **3** (see Figure 5 inset). As seen after a heat–cool–heat sequence, the melting point remains extremely stable (single endotherm at 86.5 °C). This is in contrast to what is generally observed, when the presence of different packing motifs and other specific intermolecular interactions (such as  $\pi$ – $\pi$  stacking) usually significantly changes the melting endotherm.<sup>6,22</sup>

The most interesting aspect of the absorption spectra is that the relative contribution of the low-energy absorbing *trans, trans* isomer has increased distinctly in the film from melt (~18%) as compared with that of the deposited crystals (~6%) (see Figure 5, inset). This experimental fact strongly suggests that the molten phase has a pronounced effect on the *cis, cis*  $\rightleftharpoons$  *trans, trans* thermal equilibrium response. Upon cooling the sample, the cohesive molecular packing is reconstructed from the supercooled melt at about 80 °C. During the lattice reconstruction, the isomeric populations are kinetically trapped, and the equilibrium response is frozen again. This becomes evident by the absence of a temperature effect on the absorption spectrum of the above sample upon cooling again down to 77 K (see Figure 5).

One seeks, therefore, a specific volume-conserving stereochemical consequence leading directly to the *cis, cis*  $\rightleftharpoons$  *trans, trans* isomeric interconversion in the softened but still congested molten state. A possible route might be rotation of the naphthalene nucleus (rotator) about the two quasi-single bonds  $C_{\text{Aryl}}\text{--O}$  simultaneously by  $\varphi \approx 180^\circ$  while the sterically hindered oligomeric chains remain nearly static. Interestingly, in this stereochemical sequence, the lack of symmetry of the ring by the 2,6- substitution leads directly to the stereoselective interconversion between the *cis, cis* and *trans, trans* configurational isomers (see Figure 6). Concerted rotation of two bonds is expected to be a high energy isomerization process. However, it is generally observed that in media with increased steric congestion, a volume-conserving, high-energy isomerization pathway might possibly reveal itself.<sup>3</sup>

To obtain an estimate of the torsional potential energy barrier,  $E_a$ , for this rotary process, at least in the gas phase, we performed fully relaxed geometry optimization at the MP2//RHF/(aug)-cc-PVDZ level of theory varying simultaneously the dihedral angles  $\varphi(C2\text{--}C3\text{--}O1\text{--}C6)$  of both molecular sides from 0° to 180° in 20° increments (see Figure 6). The calculations predict a barrier of 32.2 kJ/mol, which is almost twice than the barrier to rotation of a methoxy group around the  $C_{\text{Aryl}}\text{--O}$  bond (16.4 kJ/mol). The hopping rate  $k = A \exp(-E_a/kT)$  between the wells minima of the *cis, cis* and *trans, trans* configurations can be estimated from an Arrhenius analysis. Using a pre-exponential factor  $A = 1.9 \times 10^{12} \text{ s}^{-1}$  (calculated from the frequency derived from the moment of inertia of a naphthalene ring rotating freely about the  $C_{\text{Aryl}}\text{--O}$  links), the hopping rate at 300 K is estimated to be  $\sim 4.7 \times 10^6 \text{ s}^{-1}$ ; this value corresponds to a half-life of the interconversion process of ~150 ns at 300 K. The calculated torsional barrier of 32.2 kJ/mol falls into the range of the literature's available data on analogues volume-conserving, molecular rotary processes.<sup>23</sup> More precisely, barriers between ~20 and ~50 kJ/mol have been reported for rotation of aryl rings, around the two linkage bonds along the long axis of symmetry, by 180° (2-fold flipping) in a free-volume, sterically unhindered environment such as the so-called molecular gyroscopes or MOFs.<sup>23</sup>

The absence of a temperature effect on the *cis, cis*  $\rightleftharpoons$  *trans, trans* equilibrium response of **3** in the solid state conclusively



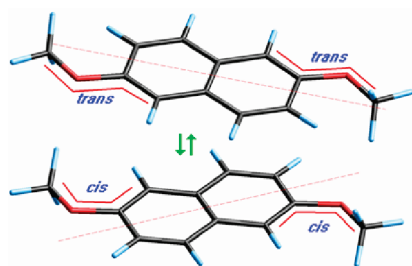


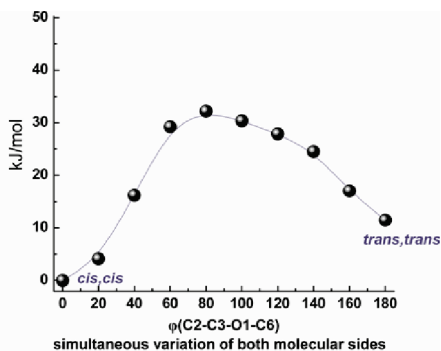
**Figure 6.** Concerted rotation about the two  $C_{\text{Aryl}}\text{--O}$  bonds leading to the interconversion between *cis, cis* and *trans, trans* isomers. The calculations showed that the naphthalene nucleus reorients between the well minima of the planar *cis, cis* and *trans, trans* configurations passing through a potential energy maximum of 32.2 kJ/mol with the methoxy groups nearly orthogonal to the plane of the aromatic subunit.

implies that such a rotary motion should be sterically strongly hindered. This can be inferred clearly if one closely inspects the crystal packing motif in Scheme 4 and, in particular, the dimeric unit shown in Scheme 5. If, for example, rotation of the naphthalene nucleus of the A unit were to occur, then one would expect that, at the orthogonal position, the close proximity ( $\sim 0.5$  Å) between the aromatic hydrogens of the A unit and the closest lying hydrogen atoms of the neighboring molecule B should lead to a repulsive state with energetically impenetrable barrier.

Finally, further evidence for the coexistence of the *cis, cis*, and *trans, trans* isomeric forms in the same crystal lattice is provided by the emission properties of crystals. As clearly seen in Figure 2b, upon excitation of the predominant *cis, cis* isomer, its own emission is not observed at all. Instead, the total emission spectrum shows extraordinary mirror symmetry with the first absorption band of the *trans, trans* isomer. Notably, this unusual photoluminescence scheme is independent of temperature and wavelength of excitation. A photochemically induced torsional transformation *cis, cis*<sup>\*</sup>  $\rightarrow$  *trans, trans*<sup>\*</sup> by no means should be excluded. Instead, because of the crystal packing arrangement of neighboring naphthalene rings displaying no  $\pi, \pi$  stacking (nonexcimeric sites), ultrafast migration of the initially formed exciton (*cis, cis*<sup>\*</sup>) may principally occur, which subsequently is trapped to a nearby site of the lowest energy *trans, trans* isomer.

## Conclusions

The results of this work provide new knowledge into the conformational diversity of a centrosymmetrically disubstituted naphthalene derivative with flexible methoxytriethyleneglycol chains in both the liquid and the solid states. Owing to the fact that the exocyclic  $C_{\text{Aryl}}\text{--O}$  linking appears to be essentially a double bond, the material can exist in discrete geometric isomers. In solution, the material exists predominantly as a mixture of two rapidly interconverting stereoisomers; namely, the thermodynamically preferred *cis, cis* and the energetically closest-lying *cis, trans* configuration. The *cis, cis* isomer was the sole observed by single crystal X-ray analysis. Optical spectroscopic methods, however, provide evidence for the presence of a low amount of the energetically highly unstable *trans, trans* stereoisomer, kinetically trapped within the nano-spaces defined by the scaffold of the predominant *cis, cis* isomeric form. The molten phase unlocks and restores the seemingly frozen thermal equilibrium response *cis, cis*  $\rightleftharpoons$  *trans, trans*. The rich isomeric composition of the ground state, taken together with the complex excited state scheme observed in the liquid<sup>18</sup> and solid phase, leads to an informative conformational



diversity that may be useful and explanatory to scientists involved in studying multicomponent functional chemical systems (e.g., molecular machines) linked with this class of compounds. Finally, we believe that the findings of this work could support efforts targeted to relate crystal scaffolds and isomerization stereoselectivity between conformationally flexible forms in cases that X-ray analysis cannot distinguish unambiguously.

## Experimental Section

**Materials.** 2-Methoxynaphthalene (**1**) and 2,6-dimethoxy naphthalene (**2**) were purchased from Fluka and Sigma Aldrich. They were first purified by vacuum sublimation and then, 2-methoxynaphthalene was recrystallized from a mixture of methanol and chloroform. Compound (**3**) was prepared according to Supporting Information Scheme S1. 2-Methyltetrahydrofuran (2MTHF) was obtained from Sigma Aldrich and was used after further purification (see also Supporting Information S2). All the other materials were obtained from Aldrich and were used as received unless otherwise stated.

**Instrumentation and Methods.** Absorption spectra were recorded on a Perkin-Elmer Lambda-16 spectrophotometer. Steady-state fluorescence spectra were accomplished by the Perkin-Elmer model LS-50B and the Edinburgh Instruments model FS-900 spectrofluorometer. Fluorescence lifetimes ( $\tau$ ) were determined using the time-correlated single-photon counter FL900 of the above Edinburgh Instruments set up, which is capable of measuring lifetimes down to 100 ps. The details for measurements at ambient and low temperatures are given in Supporting Information S2. Quantum mechanical calculations were performed using the commercial computational program HyperChem version 8.0 for windows. All computer fits and simulations, except those of time-resolved experiments, were performed using the program "Micro Math Scientist for Windows" version 2.01, of Micro Math.

**X-ray Crystal Structure Determination.** Slow evaporation of a solution of **3** in a mixture of chloroform and *n*-heptane yielded colorless prismatic single crystals. A crystal with approximate dimensions  $0.05 \times 0.50 \times 0.55$  mm was mounted in air. Diffraction measurements were made on a Rigaku R-AXIS SPIDER Image Plate diffractometer using graphite monochromated Cu K $\alpha$  radiation. Data collection ( $\omega$ -scans) and processing (cell refinement, data reduction and empirical absorption correction) were performed using the CrystalClear program package.<sup>24</sup> The structure was solved by direct methods using SHELXS-97<sup>25</sup> and refined by full-matrix least-squares techniques on  $F^2$  with SHELXL-97.<sup>27</sup> Important crystallographic data are listed in Table 4. Further experimental crystallographic details for **3**:  $2\theta_{\text{max}} = 136^\circ$ ; reflections collected/unique/used,

**TABLE 4: Crystallographic Data for Compound 3**

formula	C <sub>24</sub> H <sub>36</sub> O <sub>8</sub>
Fw	452.53
space group	<i>P</i> 2 <sub>1</sub> / <i>a</i>
<i>T</i> , °C	293
$\lambda$ , Å	Cu K $\alpha$ (1.5418 Å)
<i>a</i> , Å	8.6041(2)
<i>b</i> , Å	7.8833(1)
<i>c</i> , Å	18.1199(3)
$\beta$ , (°)	101.1297(8)
<i>V</i> , Å <sup>3</sup>	1205.93(4)
<i>Z</i>	2
$\rho_{\text{calcd}}$ , g cm <sup>-3</sup>	1.246
$\mu$ , (Cu K $\alpha$ ) mm <sup>-1</sup>	0.765
<i>R</i> 1 <sup>a</sup>	0.0579 <sup>b</sup>
<i>wR</i> 2 <sup>a</sup>	0.1666 <sup>b</sup>

<sup>a</sup>  $w = 1/[\sigma^2(F_o^2) + (aP)^2 + bP]$  and  $P = (\max(F_o^2, 0) + 2F_c^2)/3$ ;  $R1 = \sum(|F_o| - |F_c|)/\sum(|F_o|)$  and  $wR2 = \{\sum[w(F_o^2 - F_c^2)^2]/\sum[w(F_o^2)^2]\}^{1/2}$ . <sup>b</sup> For 1818 reflections with  $I > 2\sigma(I)$ .

8010/2087 [ $R_{\text{int}} = 0.0356$ ]/2087; 199 parameters refined; ( $\Delta/\sigma$ )<sub>max</sub> = 0.000; ( $\Delta\rho$ )<sub>max</sub>/ $(\Delta\rho)$ <sub>min</sub> = 0.0591/−0.0536 e/Å<sup>3</sup>; *R*1/*wR*2 (for all data), 0.0631/0.1718. Hydrogen atoms were either located by difference maps and were refined isotropically or were introduced at calculated positions as riding on bonded atoms. All non-hydrogen atoms were refined anisotropically.

**Acknowledgment.** We thank Dr. C. L. Chochois for assistance with the synthetic procedure of compound 3.

**Supporting Information Available:** Synthetic procedure of compound 3 (S1), details for measurements at ambient and low temperatures (S2), and additional references (S3). This material is available free of charge via the Internet at <http://pubs.acs.org>.

## References and Notes

- (1) Szemik-Hojniak, A.; Zwier, J. M.; Buma, W. J.; Bursi, R.; van der Waals, J. H. *J. Am. Chem. Soc.* **1998**, *120*, 4840–4844.
- (2) Khuong, T. A. V.; Zepeda, G.; Sanrame, C. N.; Dang, H.; Bartberger, M. D.; Houk, K. N.; Garcia-Garibay, M. A. *J. Am. Chem. Soc.* **2004**, *126*, 14778.
- (3) Liu, R. S. H.; Hammond, G. S. *Acc. Chem. Res.* **2005**, *38*, 396.

- (4) Balomenou, I.; Pistolis, G. *J. Phys. Chem. B* **2010**, *114*, 780.
- (5) Hellings, M.; Engelborghs, Y.; Deckmyn, H.; Vanhoorelbeke, K.; Schiphorst, M. E.; Akkerman, J. W. N.; De Maeyer, M. *Proteins* **2004**, *57*, 596.
- (6) Bernstein, J. *Polymorphism in Molecular Crystals*; Oxford University Press Inc.: New York, 2002.
- (7) Robert, S. H.; Liu, R. S. H.; Hammond, G. S.; Mirzadegan, T. *Proc. Natl. Acad. Sci. U.S.A.* **2005**, *102*, 10783.
- (8) Anderson, S.; Srajer, V.; Moffat, K. *Photochem. Photobiol.* **2004**, *80*, 7.
- (9) Hellings, M.; De Maeyer, M.; Verheyden, S.; Hao, Q.; Van Damme, E. J. M.; Peumans, W. J.; Engelborghs, Y. *Biophysics* **2003**, *85*, 1894–1902.
- (10) Beierlein, F. R.; Othersen, O. G.; Lanig, H.; Schneider, S.; Clark, T. *J. Am. Chem. Soc.* **2006**, *128*, 5143.
- (11) Kay, E. R.; Leigh, D. A.; Zerbetto, F. *Angew. Chem., Int. Ed.* **2007**, *46*, 72–191.
- (12) Janssen, P. G. A.; Jabbari-Farouji, S.; Surin, M.; Vila, X.; Gielen, J. C.; de Greef, T. F. A.; Vos, M. R. J.; Bomans, P. H. H.; Sommerdijk, N. A. J. M.; Christianen, P. C. M.; Leclere, P.; Lazzaroni, R.; van der Schoot, P.; Meijer, E. W.; Schenning, A. P. H. J. *J. Am. Chem. Soc.* **2009**, *131*, 1222.
- (13) (a) Troxler, T.; Pryor, B. A.; Topp, M. R. *Chem. Phys. Lett.* **1997**, *274*, 71. (b) Troxler, T. *J. Phys. Chem. A* **1998**, *102*, 4775. (c) Johnson, J. R.; Jordan, K. D.; Plusquellic, D. F.; Pratt, D. W. *J. Chem. Phys.* **1990**, *93*, 2258.
- (14) Balomenou, I.; Pistolis, G. *J. Am. Chem. Soc.* **2007**, *129*, 13247.
- (15) Bolte, M.; Bauch, C. *Acta Crystallogr., Sect. C* **1998**, 1862.
- (16) Dunning, T. H. *J. Chem. Phys.* **1989**, *90*, 1007.
- (17) *Handbook of Chemistry and Physics*, 70th ed.; CRC Press: Boca Raton, 1989.
- (18) Balomenou, I.; Pistolis, G. *Chem.—Eur. J.* **2009**, *15*, 4228.
- (19) Strickler, S. J.; Berg, R. A. *J. Chem. Phys.* **1962**, *37*, 814.
- (20) Pope, M.; Swenberg, C. E. *Electronic Processes in Organic Crystals and Polymers*, 2nd. Ed.; Oxford University Press: New York, 1999.
- (21) Nangia, A. *Acc. Chem. Res.* **2008**, *41*, 595.
- (22) Clark, C. G.; Floudas, G. A.; Lee, Y. J.; Graf, R.; Spiess, W. H.; Müllen, K. *J. Am. Chem. Soc.* **2009**, *131*, 8537.
- (23) (a) Khuong, T. A. V.; Nunez, J. E.; Godinez, C. E.; Garcia-Garibay, M. A. *Acc. Chem. Res.* **2006**, *39*, 413. (b) Gould, S. L.; Tranchemontagne, D.; Yaghi, O. M.; Garcia-Garibay, M. A. *J. Am. Chem. Soc.* **2008**, *130*, 3246.
- (24) Rigaku/MS; *CrystalClear*, Rigaku/MS Inc., The Woodlands, TX, 2005.
- (25) Sheldrick, G. M., SHELXS-97: Structure Solving Program, University of Göttingen: Göttingen, Germany, 1997.
- (26) Sheldrick, G. M., SHELXL-97: Crystal Structure Refinement Program, University of Göttingen: Göttingen, Germany, 1997.

JP103095Z